Cavitation by spall fracture of solid walls in liquids

V. Mikulich, Ch. Brücker

Institute for Mechanics and Fluid Dynamics, TU Bergakademie Freiberg, Lampadiusstr. 4, D-09596 Freiberg, Germany

Tel.: + 493731394133

Fax.: + 493731393455

vladimir.mikulich@imfd.tu-freiberg.de

http://tu-freiberg.de/fakult4/imfd/fluid/

Abstract

Experiments are carried out to investigate the cavitation process induced by the spill-off from material from a surface in a liquid environment. Therefore a simplified physical model was designed which allows the optical observation of the process next to a transparent glass rod submerged in a liquid where the rod is forced to fracture at a pre-defined groove. High-speed shadow-imaging and refractive index matching allow observation of the dynamics of the cavitation generation and cavitation bubble breakdown together with the flow. The results show that the initial phase of spill-off is a vertical lift-off of the rod from the surface that is normal to the direction of pendulum impact. A cavitation bubble is immediately formed during spill-off process and grows in size until lateral motion of the rod sets in. While the rod is transported away, the bubble shrinks into hyperbolic shape and finally collapses. This process is regarded as one contributing factor to the high efficiency of hydro-abrasive wear.

Keywords: Cavitation, spall fracture, collapse, model experiments

1 Introduction

At deformation of condensed matter under stress and strain micro- and macro-cavities can occur. This phenomenon is called cavitation. The term cavitation is used both in mechanics of liquids and in mechanics of different solid materials. In engineering applications cavitation is often observed e.g. in bearings and gears which was the motivation for intensive studies in real systems and on physical models at various methods imposing the strain and shear in the liquid, for a review see Pernik 1966; Knapp et al. 1970; Franc et al. 2004; Caupin et al. 2006. Much attention is therefore paid in the literature to cavitation in the field of tribology (cavitation wear) where this phenomenon is investigated under the combined aspect of solid- and fluid mechanics (Buravova et al. 2011). As

concluded by Reiner (1958), from a rheological point of view, there is rather a quantitative than a qualitative difference in liquids and solids. Joseph (1998) even applied the strength hypotheses of solid mechanics to describe cavitation in liquids.

Cavitation in liquids is often initiated by the presence of cavitation nuclei in the liquid. These are free gas micro-bubbles or solid micro-particles in the volume of the liquid. Even in pure distilled water bubbles and particles of size of ~ 1 μm are present, see Kedrinskii 1989. This fact explains why in experiments cavitation often occurs before the critical conditions determined from theory are reached. Once cavitation bubbles are formed in the liquid they tend to collapse rapidly when the pressure rises again. An important consequence of the collapse is the induced impact on nearby solid surfaces. Therefore, in many practical cases cavitation causes the destruction of work surfaces. Due to the collapse of the bubble a liquid micro-jet is formed that induces a concentrated impact on the nearby surface (Lauterborn 1980). In addition, the collapse of the bubble in the liquid induces a hydrodynamic shock wave which may deform the material near the surface. Repeated dynamic impact of bubble collapse on the same area of the surface leads to the formation of micro-cracks, their growth and a subsequently chipping off of material from the wall (Buravova 1998). The size and shape of eroded particles depends on the physico-mechanical properties of the material as well as on the nature and duration of exposure to the surface. For example, Abouel-Kasem et al. (2009) observed eroded particles with a size up to 360 μm. If micro-particles are present in the liquid, either generated from cavitation erosion or as added abrasive material, the cavitation induced damage may reinforce itself. This is called hydro-abrasive wear. Pipe ducts, turbines and many other technical systems are exposed to this type of wear. The wear rate is significantly higher than the cavitation induced wear in pure liquids (Hengyun et al. 1986, Zhao et al. 1993, Huang et al. 1996, Chen et al. 2009). Both cavitation induced bubble collapse and abrasive particles impact on the solid surface, thus forming longitudinal, radial and lateral cracks, which then lead to material splitting off (see Figure 1).

Up to now most of the studies focused so far on the failure of a surface as a consequence of cavitation, however there is not much knowledge about the process that occurs in the liquid when a part of the surface wall is splitting off

from the main body. In this case a cavity is formed in the gap between the split particle and the newly formed surface of the material. This cavitation may undergo collapse or survive as a micro-bubble in the liquid and may form a new nucleus. Earlier experimental studies of cavitation in a liquid in a small gap were made with a sphereimpacting with a surface (Davis et al. 2002, Kantak et al. 2004, Mansoor et al. 2014, Marston et al. 2011), a sphere rolling over a surface (Ashmore et al. 2005, Prokunin et al. 2006), an elastic cylinder hitting a wall (Chen et al. 1992) and two solid walls separating from each other (Washio et al. 2008). In all studies was the gap between the separated body and the surface wall filled with a layer of liquid in which cavitation occurs. In (Chen et al. 1992) cavitation was also investigated at separation of not wetted, hydrophobic surfaces. In the present study the authors demonstrate a simplified physical model of a breaking rod to study the process of formation of cavitation in the gap between the spalling-off body and the surface wall in a liquid. The process simulates the situation in wire sawing of crystalline silicon ingots, which is the technological background of the study. This application was chosen after first indications were found in a previous study of the authors that cavitation might occur in wire sawing and may play an important role in the dynamics of the abrasive process (Mikulich et al. 2013).

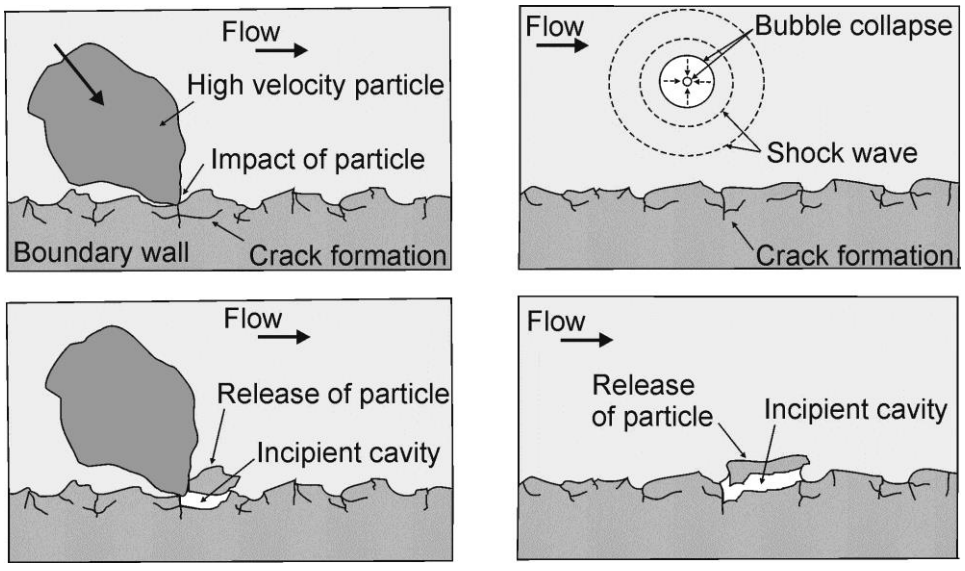

Fig. 1 Schematic diagram of chip and cavity growth during particle impact or cavitation

2 Experimental setup and conditions

The real process of interest is the so called wire sawing of crystalline silicon ingots, where suspensions of particles (slurries) in the carrier fluid (polyethylene

glycol with kinematic viscosity $\nu=19{,}17\cdot10^{-6}$ m^2 s^{-1} , are used to support the micro-mechanical removal and to ensure the transport of the particles. Cutting speed of the wire relative to the ingot is of order up to V=20 m/s and eroded particles size is up to L = 3µm. In our experiments, we use an enlarged model of a surface roughness element as a fracture sample in form of a transparent glass rod (D =1 mm, L =15 mm) submerged in glycerol. Experiments were conducted in a controlled temperature room at 20°C. The physical model (all values for the model are given in subscript "m") allows the observation of a chipping-off process of the glass-rod from the wall under defined boundary conditions in the liquid, see Fig. 2.

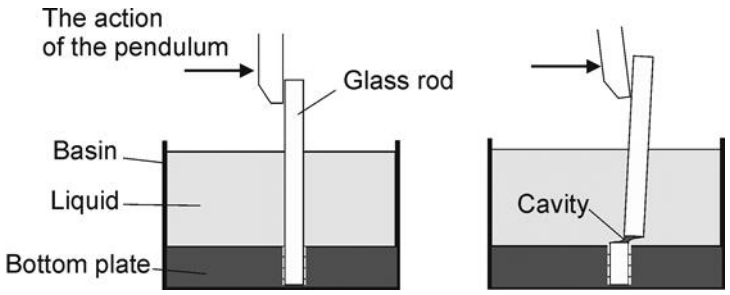

a)

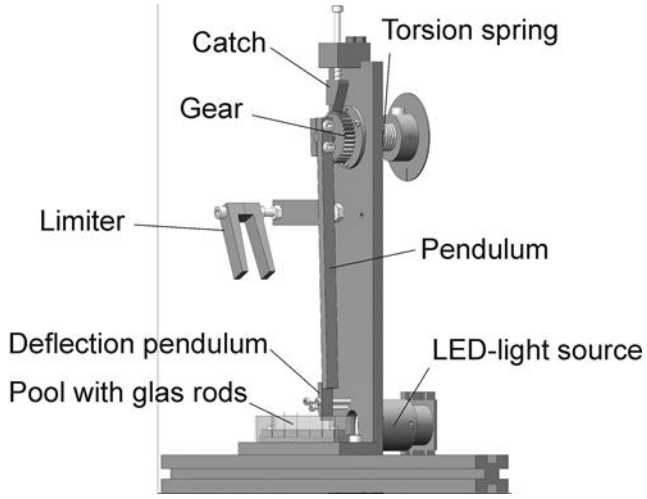

b)

Fig. 2 a Scheme of the test procedure, b Schematic of the experimental apparatus

The fracture process is enforced with a pendulum of a striking mechanism driven by a torsion spring. After release of the pendulum it strikes a small lever at a velocity of V_m=4.64m/s which transfers the impulse of the pendulum to the tip of the glass rod. The impact height is 7.5mm above the rod fixation and the filling

level of the basin is 5mm. The bottom of the glass rod is fixed in bore at the bottom wall and glued with epoxy. In order to provoke a defined position of fracture along the rod axis, a stress concentrator in form of a circumferential groove was made in the rod close to the bottom using a diamond wire. Shock loading of the glass rod leads to its fracture by bending and cracking in the groove near to the bottom plate. The development of main cracks is known to occur at speeds approaching the speed of sound propagation in the material (Roberts et al. 1954). Since we are interested in the flow around the rod during the spill-off process the system is represented by the non-dimensional Reynolds-number $Re = V L / \nu$ where V is the characteristic impact velocity, L is the characteristic length scale, ν is the kinematic viscosity of the fluid. In the real process, the Reynolds number of the flow around the spilled-off particle is in the range of Re = 3-4. In our model experiments the conditions are adapted to the same Reynolds-number with values of impact velocity V_m=4,64 ms^{-1} , the diameter of the rod as the characteristic length scale L_m=1·10^{-3} m and the viscosity of glycerol as the carrier liquid with ν_m=1,18·10^{-3} m^2s^{-1} (at 20°C room temperature). The cavitation number *Ca* could not be kept as low as in the real process, see further below. In addition, the enlarged model underestimates any capillary effects that might be of importance for the real process. For further discussion see chapter 4.
The fracture process is recorded from the side using a high-speed camera (Phantom V12.1 1280×800 CMOS sensor, 50000 fps at 400×250 px^2) equipped with a long-range microscope lens (M = 4). A LED-light source operating in continuous mode is used for illumination with a lens system. The images were obtained in backlight conditions and the region of interest is arranged in the small depth of focus of the microscope.

3 Experimental observations

Figure 3 shows a sequence of the images during an exemplary experiment. Due to refractive index matching between the liquid and the glass the images are not disturbed by any reflections or spots. In addition, the cavity is clearly seen by the dark shadow against the bright background as typical for shadow-imaging of gas bubbles in liquids. The dimensions of the images are 1860×1160 μm^2 in physical space and the recorded period represented a total time-span of 270 µs. One can clearly recognize the position of the rod and the development of the cavity after

the spill-off process. In the first 30µs the rod moves almost in vertical direction and the cavity increases. Accumulated elastic energy during the preceding deformation of the rod leads to a very rapid separation and displacement of the rod relative to the base after fracture. In the liquid between the rod and the base a cavity is formed. Then the transversal motion of the rod sets in which deforms the cavity in lateral direction. At the end of the recorded time-span the cavitation collapses (Fig. 3 at time step 9). To determine the kinematics of the broken rod, the existing image data were analyzed using the coordinates of two characteristic marker points (points 1 and 2, Figure 3) along the rod. Fig. 4 illustrates the results in form of profiles of the coordinates and the velocity components (V_{1x},V_{1y}) and (V_{2x},V_{2y}) for the two points on the rod respectively. The vertical velocity is nearly constant from the beginning over the whole time-span with an average value of 1m/s. In comparison, the transversal velocity starts with a delay of t=30µs but then rises sharply to a peak velocity of about 8m/s at 90 µs. Thereafter, the velocity falls off in an oscillating manner to lower values. In general, the similar values of the velocities at the two marker points indicate that the motion does not involve a rotation of the rod.

The observed oscillations are linked with the excited vibrations of the rod. Accumulated strain in the elastic rod leads to the fact that after fracture there are "free" flexural and longitudinal damped vibrations of a certain frequency and amplitude. In our case, the period of the flexural vibration of the rod is measured from Fig. 4 to approximately T = 90 µs, which corresponds to a vibration frequency of $f \approx 11$ kHz. Due to the damping influence of the fluid, the experimentally observed frequency of vibration of the rod is about two times less than the theoretical natural frequency of flexural vibrations of a free rod $f_n \approx 21{,}2$ kHz in vacuum calculated by the equation

$$f_n = \frac{S^2}{2\pi l^2}\sqrt{\frac{EJ}{A\rho}}$$

where S=4,73 - shape factor of 1st vibrational mode, l =15mm - length of the rod, E=64·10^3 Nmm^{-2} - the Young's modulus of glass, J and A - moment of inertia and area of the cross section of the rod, ρ=2,23 gcm^{-3} – glass density. This hints at the damping that the high-viscosity fluid is imposing on the glass motion. Not

only is the viscous friction responsible for the decrease in frequency but also the added mass that must be taken into account when the rod and the nearby fluid is set into motion. Both effects contribute to the reduction of the natural frequency in the liquid.

The diameter *d* of the cavity is measured as the horizontal width of the dark area in the gap between the lower surface of the moving rod and the wall. The volume of the cavity shrinks mainly in this direction which is parallel to the fracture surface. Temporal variation of the *d* is additionally shown in Fig. 4. The bubble disappears with a nearly constant shrinking rate within a time-span of 180μs.

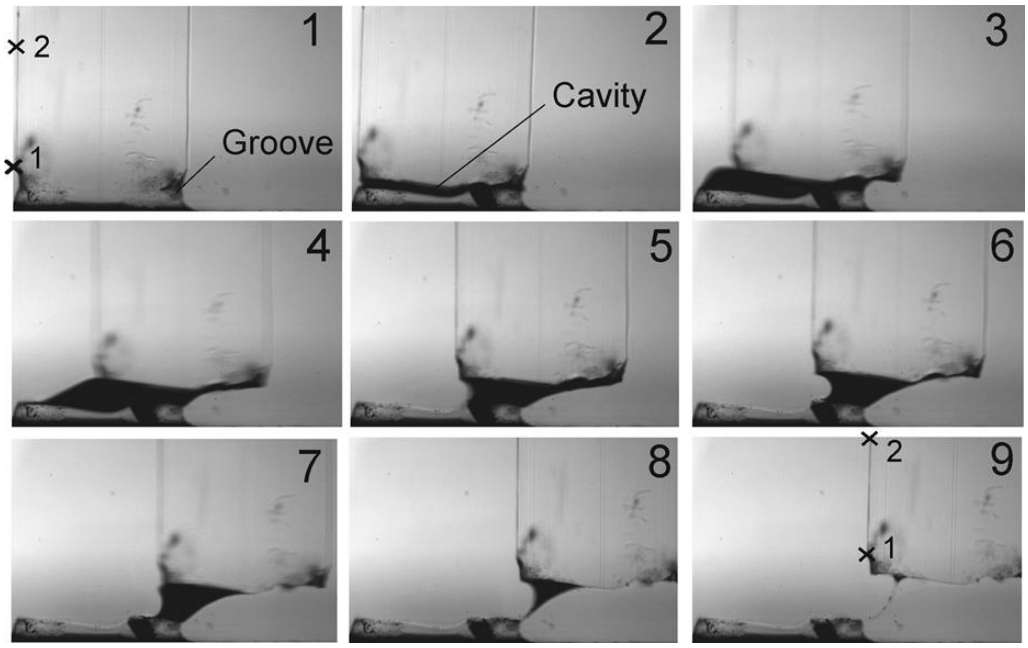

Fig. 3 Typical sequence for observed cavitation process (Δt=30 μs). The marker numbers highlight the locations where the rod displacements vectors are measured in images

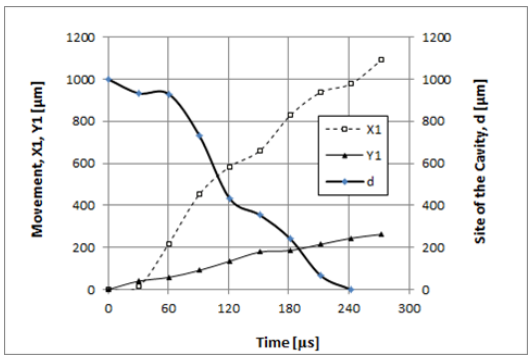

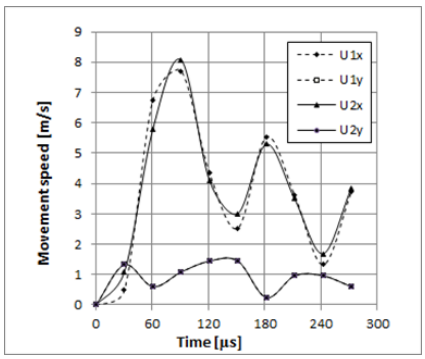

Fig.4 Left: observed marker coordinates and size of the cavity over the course of rod spill-off; right: derived velocity in the focal plane (x-direction is in impact direction, y-direction is normal to the wall)

Induced fluid motion in the region of the fracture and next to the cavity is in principle a superposition of several separate phenomena: the pressure distribution in the liquid and the cavity, the internal friction in the fluid, inertial and capillary effects (surface tension), the wettability of the fracture surface, etc. These interacting phenomena have impact on the flow and the kinematics. Flow is studied by adding small tracer particles of 10-30 µm diameter in size to the liquid and imaging their motion within the focal plane by defined exposure time of 20 µs (particle tracing). Figure 5 shows the sequence of events for an exemplary experiment.

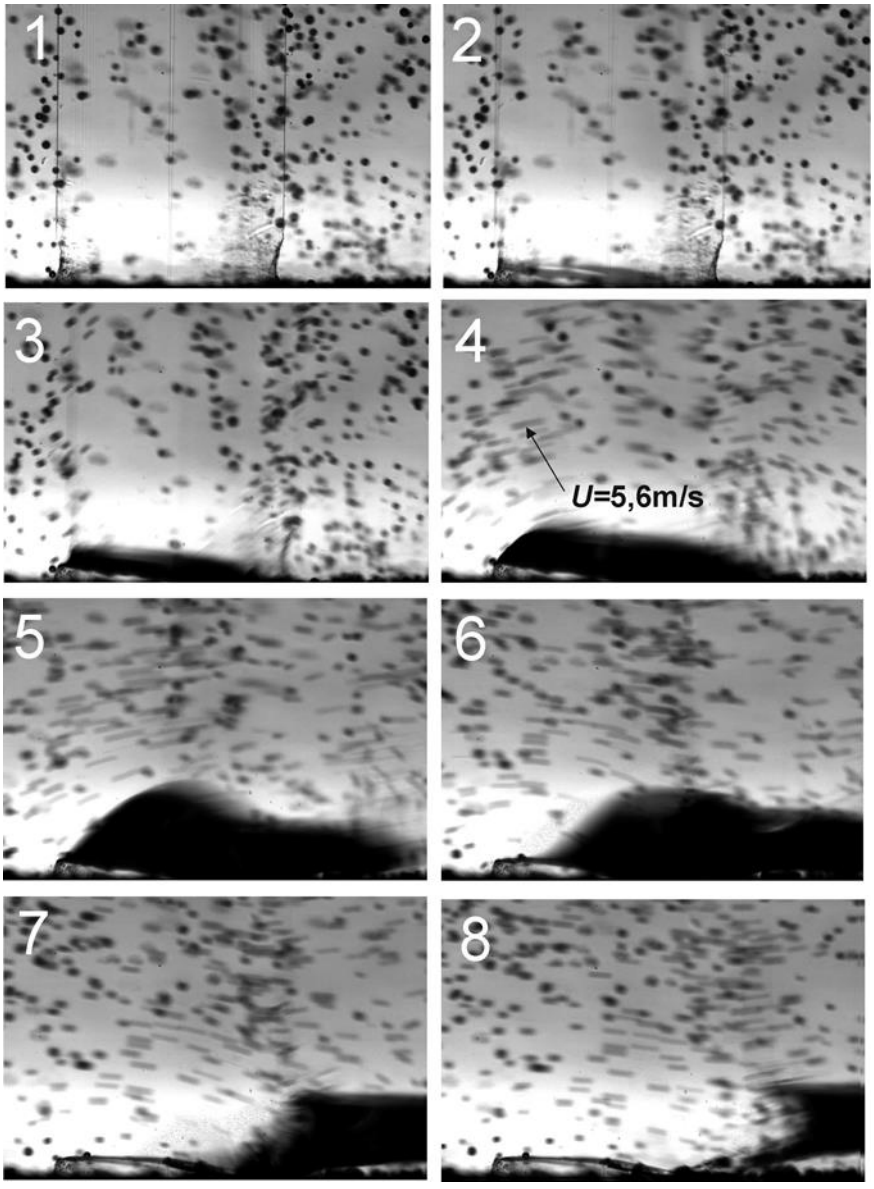

Fig.5 Cavitation evolution sequence (Δt=30μs). The exposure time for each frame is 20 μs

The position of the rod just prior to impact is shown in Figure 5.1. In figure 5.2 the fracture process is already completed and the cylinder begins to move. The contours of the glass rod are only visible in these first two pictures, while for the later time the motion blur is so high that it hinders the detection of the rod edges. In figures 5.3 and 5.4 the rod is accelerated further, this results in acceleration of the adherent fluid. In the left area of both images a linear motion of the fluid is visible. The flow follows the rod movement and seemingly does not respond to the resulting negative pressure in cavity in the early phase. Later at time t = 150μs (Fig. 5.6) the cavitation bubble is now starting to collapse. The low pressure of the cavity now progressively changes the direction of liquid flow and more and more fluid is filling the shrinking cavity.

A close-up view of the cavity region in clean fluid is shown in Fig. 6. When filling the cavity with liquid the boundary surface of the cavity region is reduced in size, loses its stability and under the influence of surface tension and of decreasing pressure in the liquid, disintegrates to form cloud cavitation seen be the large number of small bubbles next to the cavity.

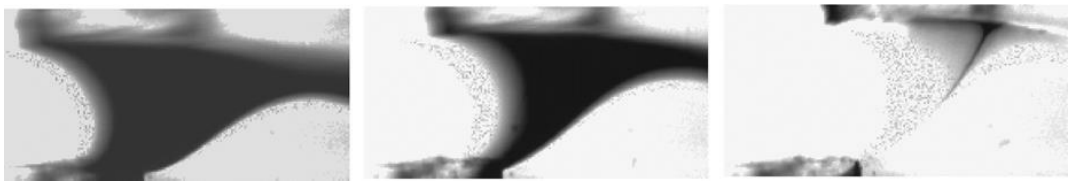

Fig.6 Three frames are presented from observed sequences illustrating the instability of the cavity collapse (Δt=24μs) and the formation of clouds of bubbles along the periphery of the larger central cavitation region.

4 Discussion and conclusions

In this work we consider a special case of cavitation which can take place at a particle splitting off from a surface of a solid body being in liquid and which has not been studied so far. This spill-off may either be a consequence of mechanical impact of a particle with the surface wall or the result of bubble collapse next to the surface and the resulting hydro-abrasive effect. Our experiments are limited to a special case of a relative large cylindrical glass rod (D =1mm) in comparison to typical sizes of eroded particles (D < 100 μm) and the results therefore cannot be

regarded as universal. The experimental conditions were rather chosen such that optical resolution and refractive index matching allow for detailed observation of the formation and breakup of the cavitation bubble with state-of-the-art high-speed imaging at 50.000 fps and resolution of 400×250 px^2. As a consequence of these constraints the parameter space of the investigations is only narrow. At least the dynamics of the fluid motion is at similar Reynolds-number of Re = O(1) as in the real process of wire cutting used in the silicon industry however, capillary effects or wetting issues however are not comparable. The vapor pressure of glycerol in our experiments is about 1mPa and the impact velocities of the striking pendulum are of the same order as typical velocities in the wire process at 10m/s. Therefore we assume a similar behavior of the cavitation emergence while the bubble collapse may differ in temporal behavior or geometrical shape.

For particles considerably smaller than in the present studies the role of capillary effects at the split-off process from surfaces can be more significant. It is expected that the smaller scale results in a faster filling of the cavity driven by the higher capillary pressure. The capillary pressure is given by the Laplace equation

$$\Delta P = \sigma \cdot \left(\frac{1}{R_1} + \frac{1}{R_2} \right)$$

where σ is the surface tension of the liquid and R_1, R_2 are the radii of the meniscus of the cavity. In our case (Fig. 3.6) $\sigma = 60 \cdot 10^{-3}$ Nm^{-1} and the radii were measured to R_1 = 0,154 mm, R_2 = 0,308mm. The resulting capillary pressure in our experiments amounts then to ΔP=584 Pa which is the level of pressure in the liquid relative to the vapor pressure in the cavitation bubble. It is obvious that with decreasing particle size the capillary forces will rise in proportional manner. With a scale factor of approx. 1/1000 of the particle diameter in the real application the capillary pressure will be then of the same order as the dynamic pressure in the liquid.

In our experiments, the cavitation number is $Ca = 2(p_r - p_v) / \rho\, U_{max}^{\,2}$ = 2,51 where p_r = 101325 Pa - reference pressure (approx. the pressure of the ambient atmosphere), p_v =0,01333 Pa - vapor pressure of the fluid (glycerol at 20ºC, see Ross& Heideger 1962), ρ = 1261 kg/m^3 - density of the fluid, U_{max} =*8* m/s - measured maximum velocity of fluid. Since *Ca* is larger than 1 the cavitation we observed is not related to flow-induced cavitation but solely driven by the spill-off process.

Considering the above limitations, the results are rather of qualitative than quantitative nature if transferred to the spill-off process at smaller scales typical in the wire cutting process. Further experiments are necessary to check our results in microscopic scale with ultra high-speed imaging at sufficient pixel resolutions which is planned for future experiments when the hardware is available in our lab. Nevertheless, the images clearly demonstrate the generation of cavitation related to the spill-off of a solid object from the surface of a wall. This process is initially coupled with a solely wall-normal motion of the cylinder after fracture although the impact was in transversal direction. It is known (Roberts et al. 1954) that the formation of the main crack in a solid occurs at a speed 0,2 - 0,37 to the speed of sound in the material. In particular, the growth rate of the main cracks in glass is at a speed of about 1500 ms^{-1}. At such high speeds of relative motion between the walls the liquid cannot fill the crack volume at the same speed due to viscous friction, therefore the spill-off process in viscous liquids is expected to generate always such a cavity. An interesting consequence of such type of spill-off cavitation is the possible self-sustained nature that the subsequent collapse of the bubble may have on the erosion process. The cavitation formed by the spill-off and the subsequent collapse can enforce the dynamic loading on the surface or the cavitation bubble can generate a new nuclei of growth of subsequent, more intensive cavitation processes induced by the presence of particles in the fluid. This might explain the strong efficiency of hydro-abrasive wear. In the present experiments we saw no effect of the tracer particles on the development of the large cavitation bubble and the formation of the cloud of smaller bubbles later in the breakup process. So under the given conditions the tracer particles do seemingly not act as nucleation kernels. However, this may change if the process is investigated at smaller scales and with particle-laden slurry as typically applied in the process of wire cutting.

Acknowledgments The studies of the wire sawing process that initiated the current work on cavitation were funded by the DFG in the project Br 1494/20-1. The authors gratefully acknowledge the support herein.

References

Abouel-Kasem A, Emara KM, Ahmed SM (2009) Characterizing cavitation erosion particles by

analysis of SEM images. Tribology International 42:130– 136

Ashmore J, Del Pino C, Mullin T (2005) Cavitation in a lubrication flow between a moving sphere and a boundary. Phys Rev Lett 94:124501

Barnocky G, Davis RH (1988) Elastohydrodynamic collision and rebound of spheres: Experimental verification. Phys Fluids 31:1324–1329

Buravova SN (1998) Surface damage as a result of cavitation erosion. Tech. Phys. 43: 1107–1110

Buravova SN, Gordopolov Yu (2011) Cavitation erosion as a kind of dynamic damage. International J. of Fracture 170(1):83-93

Caupin F, Herbert E (2006) Cavitation in water: a review. C. R. Physique 7:1000–1017

Chen H, Wang J, Chen D (2009). Cavitation damages on solid surfaces in suspensions containing spherical and irregular microparticles. Wear 266 (1-2) 345-348

Chen YL, Kuhl T, Israelachvili J (1992) Mechanism of cavitation damage in thin liquid films: collapse damage vs. inception damage. Wear 153:31–51

Davis RH, Rager DA, Good BT (2002) Elastohydrodynamic rebound of spheres from coated surfaces. J Fluid Mech 468:107–119

Franc JP, Michel JM (2004) Fundamentals of Cavitation. Kluwer, Dordrecht

Hengyun J, Fengzhen Z, Shiyun L, Chenzhao H (1986) The role of sand particles on the rapid destruction of the cavitation zone of hydraulic turbines. Wear 112: 199–205

Huang S, Ihara A (1996) Effects of solid particle properties on cavitation erosion in solid–water mixture. J. Fluids Eng. 118: 749-755

Joseph DD (1998) Cavitation and the state of stress in a flowing liquid. J Fluid Mech 366:367–378

Kantak AA, Davis RH (2004) Oblique collisions and rebound of spheres from a wetted surface. J Fluid Mech 509:63–81

Kedrinskii VK (1989) On relaxation of tensile stresses in cavitating liquid. Proc. of the 13th Intern. congress on acoustics, Beograd, Sabac: Dragan Srnic Press 1:327–330

Knapp RT, Daily JW, Hammitt FG (1970) Cavitation. McGraw-Hill Book Company Ed.

Lauterborn W (1980) Cavitation and Inhomogeneities in Underwater Acoustics. Springer, Heidelberg

Mansoor MM, Uddin J, Marston JO, Vakarelski IU, Thoroddsen ST (2014) The onset of cavitation during the collision of a sphere with a wetted surface. Exp Fluids 55:1648

Marston JO, Yong W, Ng WK, Tan RBH, Thoroddsen ST (2011a) Cavitation structures formed during the rebound of a sphere from a wetted surface. Exp Fluids 50:729–746

Mikulich V, Brücker Ch, Chaves H (2013) Study of hydrodynamic mechanisms of wire sawing. Advanced Methods and Technologies for Materials Development and Processing, September 18-20, Minsk, Belarus

Pernik AD (1966) Problems of cavitation. Sudostroenie Publishing House, Leningrad (Russia), 439 p

Prokunin AN, Slavin RV (2006) Cavitation-induced particle-wall interactions in Newtonian and non-Newtonian fluids. Rheol Acta 45:348

Reiner M (1958) Rheology. Springer-Verlag, Berlin

Roberts DK, Wells AA (1954) The velocity of brittle fracture. Engineering 171:820-821

Ross GR, Heideger WJ (1962) Vapor Pressure of Glycerol. J. of Chem. & Engin. Data 7:505-507

Seddon JRT, Mullin T (2008) Cavitation in anisotropic fluids. Phys Fluids 20:023102

Washio S, Takahashi S, Murakami K, Tada T, Deguchi S (2008) Cavity generation by accelerated relative motions between solid walls contacting in liquid. Proc. IMechE, Journal of Mechanical Engineering Science 222(C):1695-1706

Zhao K, Gu CQ, Shen FS, Lou BZ (1993) Study on mechanism of combined action of abrasion and cavitation erosion on some engineering steels. Wear 162–164:811–819